Rotor-wing interaction phenomena for the ERICA tilt-wing rotorcraft configuration in the DNW-LLF wind tunnel

Anton de Bruin (anton.de.bruin@nlr.nl, NLR, Voorsterweg 31, 8316PR Marknesse, the Netherlands),
Oliver Schneider (oliver.schneider@dlr.de, DLR, Lilienthalplatz 7, 38108 Braunschweig, Germany)

Abstract

As part of the EU co-funded NICETRIP project a 1:5 scale model was tested in the 9.5x9.5 m^2 test section of the low speed DNW-LLF wind tunnel in June-July 2013 (see Ref. 1). The model design and manufacturing was largely done by NLR, with inputs from TsAGI (fuselage shells), ONERA (rotor balances and blade design) and Eurocopter (rotor hub design). Model pre-testing, including ground vibration tests and model control in the wind tunnel, was done by DLR. The overall project was led by Agusta Westland.

The test matrix consisted of 7 trimmed conditions in helicopter; conversion & aircraft mode. For each trimmed condition a comprehensive number of variations (incidence, sideslip, nacelles, tilting outboard wing angles, flaps, flaperons, rudder and elevator angles, collective and cyclic blade pitch angle settings) were performed in order to provide data for the flight dynamic model data-base. In total, over 400 different flight conditions, including an exploration towards the boundary of the conversion corridor, were measured. The model has a wing span of 3 m and two 1.48 m diameter rotors and is heavily instrumented. Model trimming was enabled by a model-pilot interface from DLR to operate 16 (!) remote controls (Ref. 2). Total forces, rotor and tail forces were measured with 6-component balances. Flaperon, flap, rudder and elevator moments were measured with one-component local balances. In addition various local loads and temperatures were measured and monitored for safety reasons. For each flight condition, over 800 parameters were recorded; consisting of about 50 parameters from balance loads, strain gauges and accelerometer measurements, flight control positions, power required and 678 static and 55 dynamic model pressures. The tests resulted in an extensive and valuable database for the validation of the ERICA tilt-wing/tilt-rotor concept.
The relatively large rotors, placed at the wing tips and operating close to the wing leading edge, create significant wing-rotor interference effects, especially during high thrust conditions. Each blade passage over the wing leading edge not only leads to a periodic loading effect on the blade, but the blade wake and blade tip vortex passage over the wing also creates periodic loading of the wing. In turn these unsteady loadings can be a driving factor for rotor and wing vibrations. In a previous paper the unsteady rotor loads and nacelle vibration levels observed during the DNW-LLF tests have been investigated (Ref. 3). In the present paper the focus will be on the steady but particularly on the unsteady pressures measured on the outer wing and their correlation with blade passage, observed vibration levels and flaperon loadings.

Introduction

The tests with the 1:5 scale model of the ERICA tilt-wing configuration were made in June 2013 in the 9.5x9.5 m^2 test section of the DNW-LLF wind tunnel up to Ma=0.17 (V=59 m/s). Prior to these tests ground vibration tests of the model were made by DLR Goettingen in order to assure a safe operation of the model. In May 2014, with the same model, also high speed tests up to Ma= 0.55 have been performed in ONERA-S1 wind tunnel (Ref. 3). The model design and manufacturing was largely done by NLR, with inputs from TsAGI (outer geometry shells) and ONERA (rotor balances and blade design). The overall project was led by Agusta Westland. The present paper only deals with the low speed DNW-LLF tests, with special emphasis on the interaction between the rotor and the wing, as reflected in the unsteady pressures on the outer wing and unsteady loads on the flaps.

Model, instrumentation and test matrix

The model has a wing span of 3 m and two 1.48 m diameter rotors placed at the wing tips. Both rotors operate at the same rotational speed (rpm) by a central gearbox, driven by two air motors. The pitch angle of the outer wing (starting at 830 mm span position) and that of the nacelles can be changed independently, but the nacelle pitch angle is always larger than that of the outer wing. A sketch showing the remote controlled movable surfaces of the model is shown in Figure 1 and model dimensions are shown in Figure 2.
The test matrix in the DNW-LLF wind tunnel included trimmed conditions in Helicopter (HC1, HC2, HC3), Conversion Corridor (CC1, CC2, CC4) and a low speed high angle of attack Aircraft mode (AC1). An overview of the trimmed conditions tested is given in Table 1. For these test points the total lift of the model is trimmed to the scaled-down full aircraft

design weight and the total drag and pitching moment are trimmed to zero.
All test conditions in DNW-LLF apply to zero altitude flight conditions. In helicopter mode the trimming is mainly done by adjusting blade collective pitch and thus rotor thrust. In aircraft mode lift is mainly controlled by aircraft pitching angle and drag by blade collective pitch control. Depending on test condition, the nacelle pitching angle varies between 0 (AC1: aircraft mode) and 90 deg (HC1: pure helicopter mode). For the trimmed conditions, a visual display of the rotor position with respect to the wing (blue lines) and with respect to the fuselage center line (red dashed line) is shown in Figure 3. The average rotor thrust and F_z force vectors are indicated by red lines, showing that max thrust is needed in helicopter mode and minimum thrust is needed in aircraft mode. A significant in-plane force component F_z is only observed for the CC4 case. Here _cy denotes a test case with and _nc a test case without cyclic pitch control. During the tests it became necessary to abstain from cyclic pitch inputs to prevent blade pitch bearing overloads. For the trimmed conditions, an overview of rotor total thrust (along rotor axis) and contribution to lift is shown in Figure 4. Figure 5 shows the different (trimmed) test conditions in velocity and nacelle pitch angle space.
The model is mounted on an internal 6-component main balance on a dorsal sting support in DNW-LLF (see Figure 6).
For each case a comprehensive number of variations (model incidence, sideslip, nacelle tilting angle, outboard wings tilting angle, flap, flaperons, rudder and elevator deflection angles and blade collective pitch angles) were performed in order to provide data for the flight dynamic model data-base. In total, over 400 different flight conditions, including an exploration towards the boundary of the conversion corridor, were measured.
The model was heavily instrumented. Model trimming and quick model changes were enabled by a model-pilot interface from DLR to operate 16 (!) remote controls for cyclic pitch of the rotor blades (2x3), rudder (1), elevator (1), outer wings (2), nacelles (2), flaperons (2) and flaps (2). The model-pilot interface is shown in Figure 7 and further details are given in Ref. 4. Total forces, rotor and tail forces were measured with 6-component balances. Flaperon, flap, rudder and elevator moments were dynamically measured with one-component local balances. In addition various local loads and temperatures were dynamically measured and monitored for safety reasons. This included measurement of blade bending and torsion moments (one blade/rotor), rotor shaft bending moment, rotor shaft torque (independent of rotor balance torque), swash plate actuator forces (2/rotor) and various accelerometer signals. For each test condition, over 800 parameters were recorded; including about 50 parameters from balance loads, strain gauges, accelerometers, flight control positions and 678 static (mainly at Left Hand (LH) side of model) and 55 dynamic pressures (only at Right Hand (RH) side of the model). All dynamic sensor signals, including rotor loads, were evaluated and stored up to the 16^{th} harmonic in amplitude and phase, using a harmonic analysis of the signals from 32 rotor revolutions.
Dynamic pressures were phase averaged over 64 rotor revolutions and averaged values were presented in 64 time steps per revolution. The tests resulted in an extensive and valuable database for the validation of the ERICA tilt-wing/tilt-rotor concept.

Due to the complexity of the model and the numerous aircraft design variables to be measured, testing was extremely challenging and many minor and larger issues were encountered and needed to be solved during the tests. Nevertheless, the test was successfully completed, thanks to the skill and experience of the integrated Agusta Westland, DNW, DLR and NLR teams.

The rotors and their operation
The counter rotating rotors of the ERICA configuration are relatively large in order to provide sufficient thrust for a vertical take-off and landing. However the aircraft may also take-off and land as a normal airplane. The rotors, designed by ONERA and Agusta Westland, are mounted at the wing tips and at a relatively short distance from the ¼ chord line (≈ 0.5 rotor radius). Combined with the fact that rotor axis pitch angle settings may be large, the rotors operate in a very non-uniform flow field under most of the testing conditions. The nominal rotor speed in all non-aircraft modes is 2765 rpm (Ma_{tip}=0.630) and in aircraft mode it is 2130 rpm (Ma_{tip}=0.485). The actual rpm during the wind tunnel test is adapted, depending on the static temperature in the wind tunnel. For the AC1 and CC4 test conditions the requested wind tunnel Mach number could not be reached (reduced to 98%), which required a small reduction in rpm to keep the design advance ratio μ.
The ERICA full scale configuration will use gimbaled rotors. However, these could not be implemented in the relatively small wind tunnel model. Instead the blades are stiff in plane (both in blade flapping and in lead/lag motion) and a swash plate operated cyclic blade pitch control was implemented to keep the

rotor in-plane moments close to zero during all test conditions. The collective and cyclic pitch of the blades of each rotor is operated through three remotely controlled actuators for setting the position of the swash plate. Collective pitch changes allow adjustment of the rotor thrust and cyclic pitch changes allow trimming to near-zero rotor in-plane moments. Unfortunately, due to problems with the blade pitch bearings (see Ref. 2), the majority of the tests were done without cyclic blade pitch control (see Table 1).

Phase averaged time signals can be reconstructed from the 1 to 8/rev recorded data. E.g. for signal *V*, having V_0 as time-mean value and V_n and ψ_n as n/rev amplitude and phase angle:

$$V(\psi) = V_0 + \sum_{n=1}^{8} V_n cos(n\psi - \psi_n)$$

It should be noted that ψ denotes the position of blade #1. The rotor azimuth position angle ψ is defined in Figure 8. The blade pitch inputs for blade #1 for the AC1_cy and CC4_cy trimmed cases are shown in Figure 9. Note that max blade pitch angle is applied near ψ=270 deg, in order to compensate for the lift loss when the blade is moving "backwards" on the tilted rotor.

Pressure sensor locations

The span wise and related rotor radial positions of the wing pressure sections are given in Table 2. Since the split between inner and outer wing lies at y=0.83 m (2y/b=0.5533), there are five sections on the outer and four sections on the inner wing. On the LH side of the wing each section has 16 pressure tabs on the upper and 12 pressure tabs on the lower side. On the RH side each section has only two static pressure tabs on the upper and lower side and five unsteady pressure sensors (including one at the leading edge), as shown in Figure 10. The unsteady pressure sensor positions are given in Table 3. The straight untwisted tapered wing has a constant airfoil and a preset angle of attack of +3 deg with respect to the fuselage centerline.

Unsteady pressures for the trimmed conditions

The magnitude of the unsteady pressures on the wing depends on the specific aircraft configuration tested. To get a first impression, all trimmed model configuration test results have been inspected. It appears that the unsteady pressures for the helicopter configurations remain quite small. For the CC1, CC2, CC4 and AC1 configurations results for the 2y/b=0.7425 wing span wise position (corresponding to r/R=0.5169 radial position) are shown in Figure 11. Clearly the largest pressure fluctuations are found for the CC4 and AC1 trimmed conditions. With reference to Figures 3-5 these are conditions with a relatively low thrust, but high wing lift. Also for the AC1 case the rotor blades pass directly along the wing leading edge, affecting the whole outer wing instantaneously. In the following the AC1 and CC4 test cases will be investigated in more detail.

Pressure data analysis for AC1 case

Figure 12 and Figure 13 show mean static pressure distributions at an inboard (LW-B) and an outboard (LT-B) wing sections for the AC1 configuration with all model settings as for the trimmed condition (see Table 1, α=10 deg), but model angle of attack α changing from 4.1 to 14.2 deg. At the higher angles of attack the flow over the wing separates, especially on the inboard wing section. For the AC1 case the rotor thrust has been varied between -40 and +750N by changing the collective blade pitch angle from 22.9 to 29.9 deg. Figure 14 shows that this variation in thrust has only a moderate effect on the mean wing pressure distributions behind the rotor.

Measured unsteady pressures (mean pressure over the entire cycle is subtracted) for various stream-wise positions on the wing of the trimmed AC1 configuration with cyclic blade pitch are shown in Figure 15. The passage of the rotor blades in front of the wing causes a clear 4/rev variation in stagnation point position, as reflected by the strong variation in wing leading edge pressures. Starting at r/R=0.8716 the pressure amplitude steadily increases for lower r/R values and it becomes largest for the r/R=0.2973 location, where it fluctuates between -1000 and +700 Pa (corresponding to about -0.45 to +0.33 in C_p). The pressure variation at r/R=0.9392 differs in character from the other LE positions. The r/R=0.9392 and r/R=0.8716 data display an opposite sign pressure peak near ψ=50 deg, probably because these locations lie at opposite sides of the helical blade tip vortex. It should be noted that for r/R≤0.872 all pressure fluctuations on the wing LE are well correlated in phase, but that this becomes less at more downstream positions. Pressure fluctuations on the x/c=0.83 wing lower side positions remain very small.

At larger thrust settings the strength of the blade tip vortex and these pressure peaks increase, as can be seen in Figure 16 and 17.

Figure 18 shows basically the same data as Figure 15, but now separately for each span-wise instead of stream-wise position. Figure 19 shows the same data for the high thrust (750 N) condition. It is found

that apart from the LE, all pressure fluctuations (even at high thrust setting) remain within +/- 300 Pa. Therefore, with a dynamic pressure of about 2100 Pa, the maximum variations in C_p are about +/- 0.14. The unsteady pressures on the wing may lead to unsteady overall loading of the wing. The spatial resolution of the unsteady pressure data is too coarse to allow an integration of overall unsteady wing loads, but CFD simulations have shown (Ref 5) that there is about a 4/rev 6% fluctuation in lift on the tilted wing for this AC1 condition. Measurements show substantial 4/rev vibration levels on the nacelles, which, just as the pressure fluctuation levels, steadily increase with thrust setting (see Figure 20). It should be noted however that the vibration characteristics of the wind tunnel model are likely different from that of a full scale aircraft.

Pressure data analysis for the CC4 case

Figure 21 and 22 compare measured unsteady pressures for trimmed CC4 configurations, both witch cyclic (Figure 21) and without cyclic pitch movement of the rotor blades (Figure 22). With cyclic blade pitch control the pressure fluctuations on the wing tend to be smaller than without cyclic blade pitch control. Cyclic blade pitch control clearly also has an effect on the shape of the pressure pulses over the wing.

With the rotor now at a different orientation and position in front of the wing than for the AC1 configuration (see Figure 3), the pressure fluctuations become less correlated along the wing span. This can be verified by comparing Figure 15 (AC1cy) and Figure 21 (CC4cy).

Concluding remarks

Tests in DNW-LLF focused on the low speed conditions in helicopter mode and on test conditions in the conversion corridor up to a high lift, low speed aircraft mode. During the tests the rotor operated under a large range of thrust and pitch angle conditions.

The tests with the highly instrumented wind tunnel model provided a large volume of data for each test point.

In the present study focus was on the unsteady pressures on the outer wings in relation to the azimuthal position of the rotor blades.

It was found that the unsteady pressures on the outer wing are largest for the AC1 and CC4 test conditions where the wing operates in relatively large lift conditions, but the rotor thrust is relatively low.

The present analysis shows the 4/rev periodic nature of the rotor induced wing pressures under a variety of rotor inflow conditions. Focus was on the trimmed reference conditions. The presented results are well suited to validate or verify existing semi-empirical or CFD methods to predict such periodic effects.

The model design and manufacture and the wind tunnel tests were made in the framework of the EU co-funded 5th Framework project NICETRIP and involved contributions from partners Agusta-Westland, DLR, NLR, ONERA and TsAGI.

References

1. A. Stabellini, A. Verna, A. Ragazzi, J. Hakkaart, A.C. de Bruin, , A.H.W. Hoeijmakers, O. Schneider, M. Przybilla, H.J. Langer, I. Philipse: “First NICETRIP Powered Wind Tunnel Tests Successfully Completed in DNW-LLF”, 70th Annual Forum of the American Helicopter Society, Montreal, Canada, 2014.

2. A.C. de Bruin, O. Schneider: “A discussion of measured static and dynamic rotor loads during testing of the ERICA Tilt-Wing rotorcraft configuration in DNW-LLF wind tunnel”, 40th European Rotorcraft Forum, Southampton, UK, 2014.

3. F. LeBrun, D. Munier, J. Decours, Ph. Beaumier: *ONERA S1MA Wind Tunnel Testing Capabilities of a Modern Tilt Rotor*, 71th Annual Forum of the American Helicopter Society, Virginia Beach,
Virginia, May 5–7, 2015.

4. O. Schneider, M. Przybilla, E. Brehl, H. Mainz, Y. Govers: *Preparation and conduction of the NICETRIP low- and high-speed wind tunnel tests*, 63th Deutscher Luft- und Raumfahrtkongress, Augsburg, 16-18 September 2014.

5. J. Decours, P. Beaumier, W. Khier, T. Kneisch, M. Valenti, L. Vigevano: Experimental validation of tilt-rotor aerodynamic predictions, 40th European Rotorcraft Forum, Southampton, UK, 2014.

COPYRIGHT STATEMENT

Test case	Ref Dpt	Ma_tip -	rpm 1/min	Ma_wt -	vel m/s	Alpa_sti deg	delAlpha deg	AngNac deg	AngWing deg	AngElev deg
AC1	2192	0.4672	2100	0.170	59.2	10.04	0.00	0.0	0.0	-19.0
CC4	2311	0.6037	2730	0.168	59.2	5.19	0.15	30.0	4.2	-5.5
CC4, no cyclics	2835	0.6080	2730	0.169	59.1	5.27	0.15	30.0	4.2	-4.5
HC2	2363	0.6227	2765	0.059	20.2	-0.53	1.44	81.0	45.9	12.1
HC2, no cyclics	2414	0.6223	2750	0.059	20.1	-3.60	1.45	86.7	46.0	12.1
CC1, no cyclics	2479	0.6239	2765	0.088	30.3	4.08	0.63	77.9	30.4	-1.3
HC3, no cyclics	2558	0.5603	2490	0.104	36.0	-5.15	0.34	86.6	18.6	15.7
CC2, no cyclics	2750	0.5590	2495	0.142	49.3	2.39	0.19	61.8	6.7	0.5
CC2_EP, no cyclics	2697	0.5567	2490	0.142	49.3	2.43	0.19	61.8	6.7	0.5
HC1, no cyclics	2867	0.6295	2790	0.000	0.0	0.02	0.00	89.9	80.0	-2.5

Table 1: Trimmed conditions for the model configurations tested in DNW-LLF wind tunnel

y [mm]	steady section name	unsteady section name	wing 2y/b	rotor r/R
280.0	LW-A		0.1867	1.6486
490.0	LW-B		0.3267	1.3649
700.0	LW-C		0.4667	1.0811
805.0	LW-D	RW-D	0.5367	0.9392
855.0	LT-A	RT-A	0.5700	0.8716
955.0	LT-B	RT_B	0.6367	0.7365
1117.5	LT-C	RT_C	0.7450	0.5169
1280.0	LT-D	RT_D	0.8533	0.2973
1380.0	LT-E	RT-E	0.9200	0.1622

Table 2: Steady (LH) and unsteady (RH) pressure section positions

Location	x/c	z/c
LE	0.0000	0.0000
upper	0.6700	0.0338
upper	0.8039	-0.0037
lower	0.8303	-0.0662

Table 3: Unsteady pressure sensor locations on RH wing

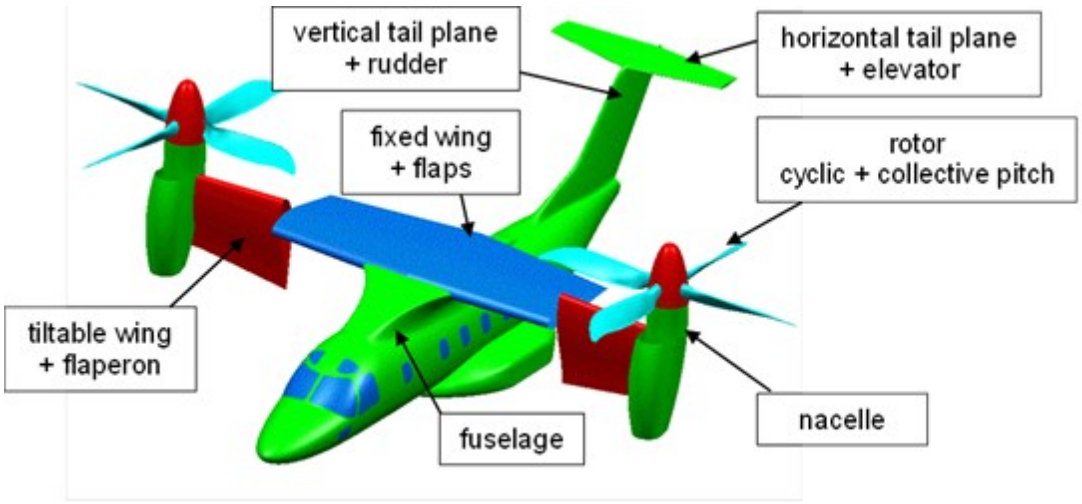

Figure 1: Sketch of ERICA configuration, showing the different model parts

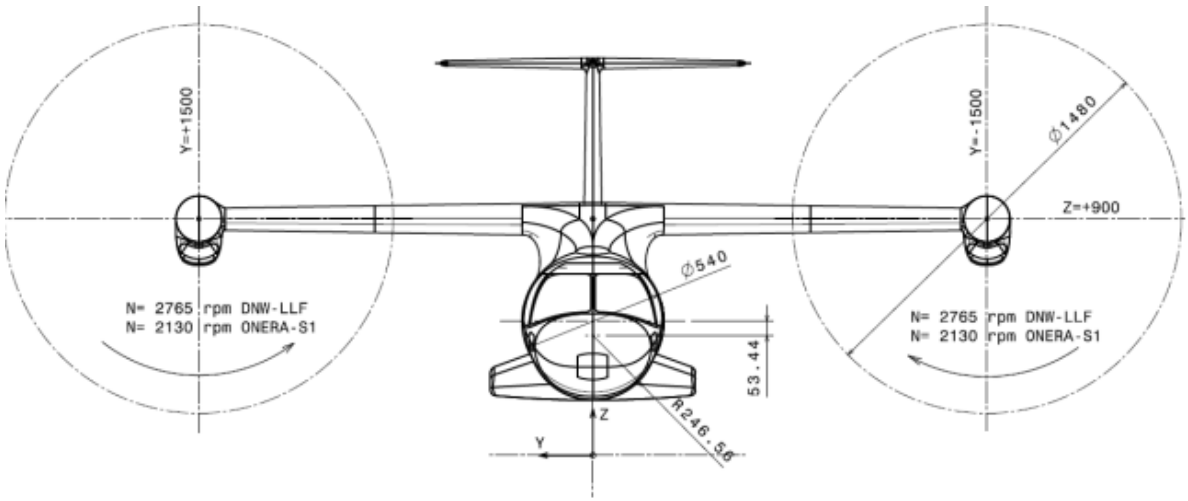

Figure 2: Front view and main dimensions (in mm) of the ERICA wind tunnel model

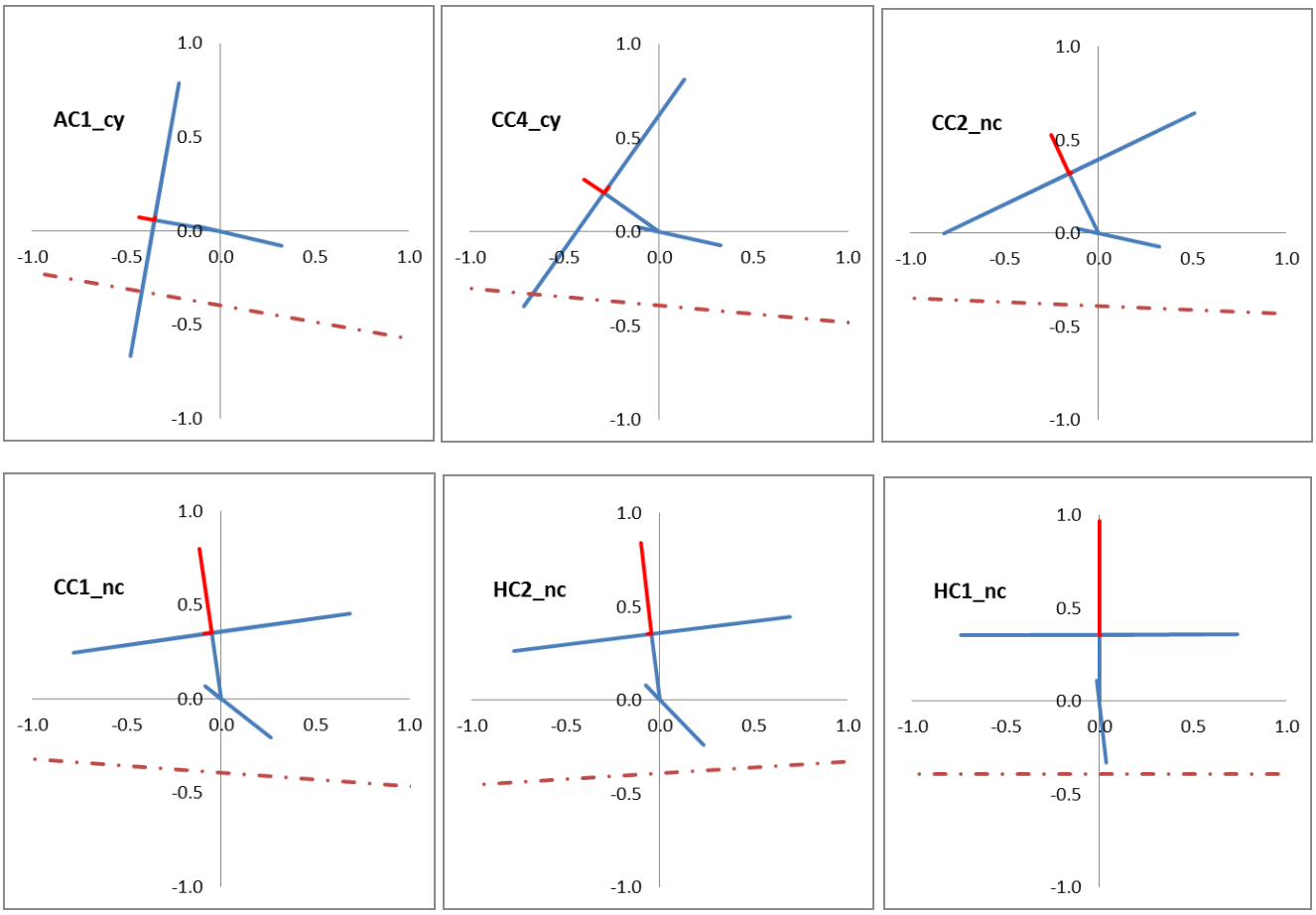

Figure 3: Sketch of rotor, rotor axis, wing tip chord and fuselage centerline (dashed) positions for the trimmed conditions (units in m). The average rotor thrust and in-plane F_z force are shown in red. The x-axis is parallel to the tunnel centerline, (x,y)=(0,0) is the position of the nacelle rotation axis at the ¼ chord line.

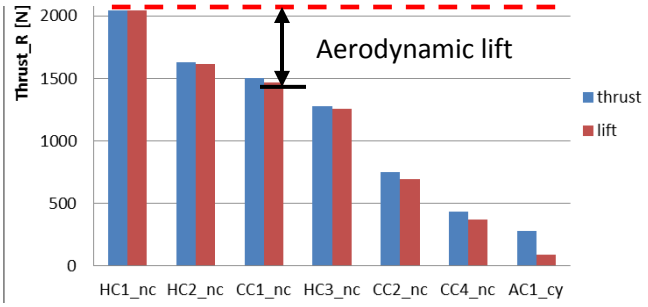

Figure 4: Rotor thrust and effect of measured thrust and F_z on lift (from RH rotor balance data).

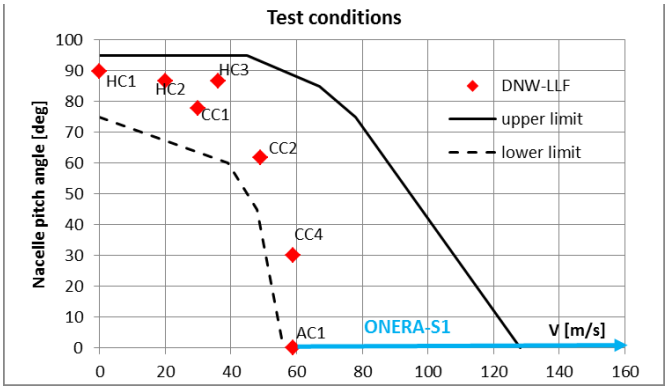

Figure 5: Tests in DNW-LLF and ONERA-S1MA

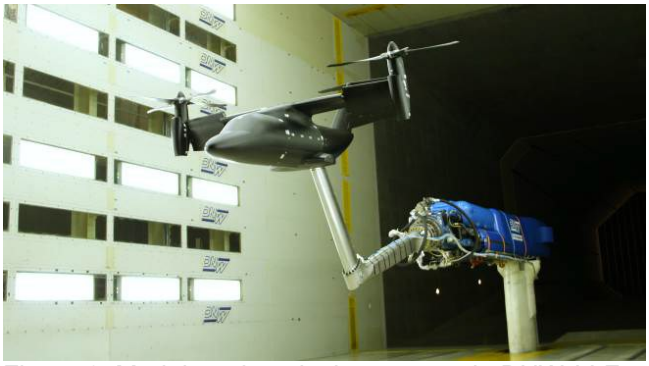

Figure 6: Model on dorsal sting support in DNW-LLF

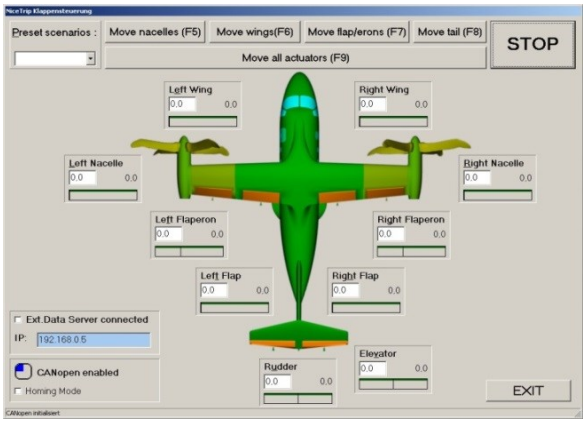

Figure 7: Actuator control interface (DLR)

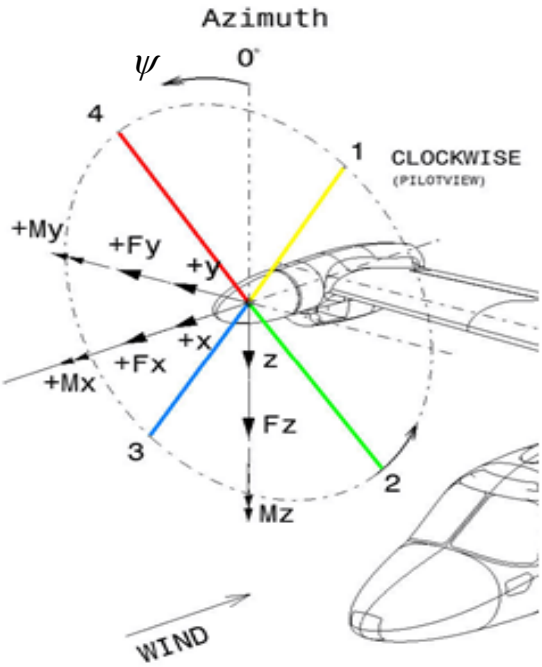

Figure 8: Definition of RH rotor axis system

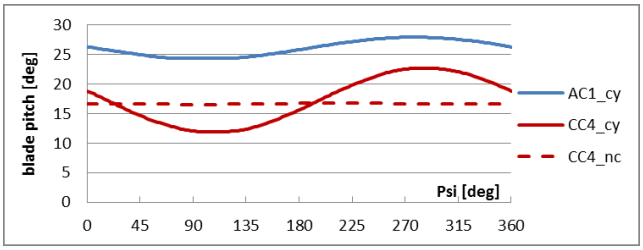

Figure 9: Blade pitch for AC1 and CC4 trimmed conditions

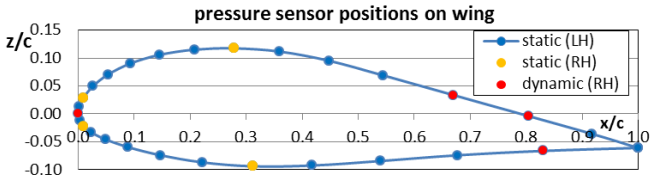

Figure 10: Pressure sensor positions on the LH and RH side of the wing

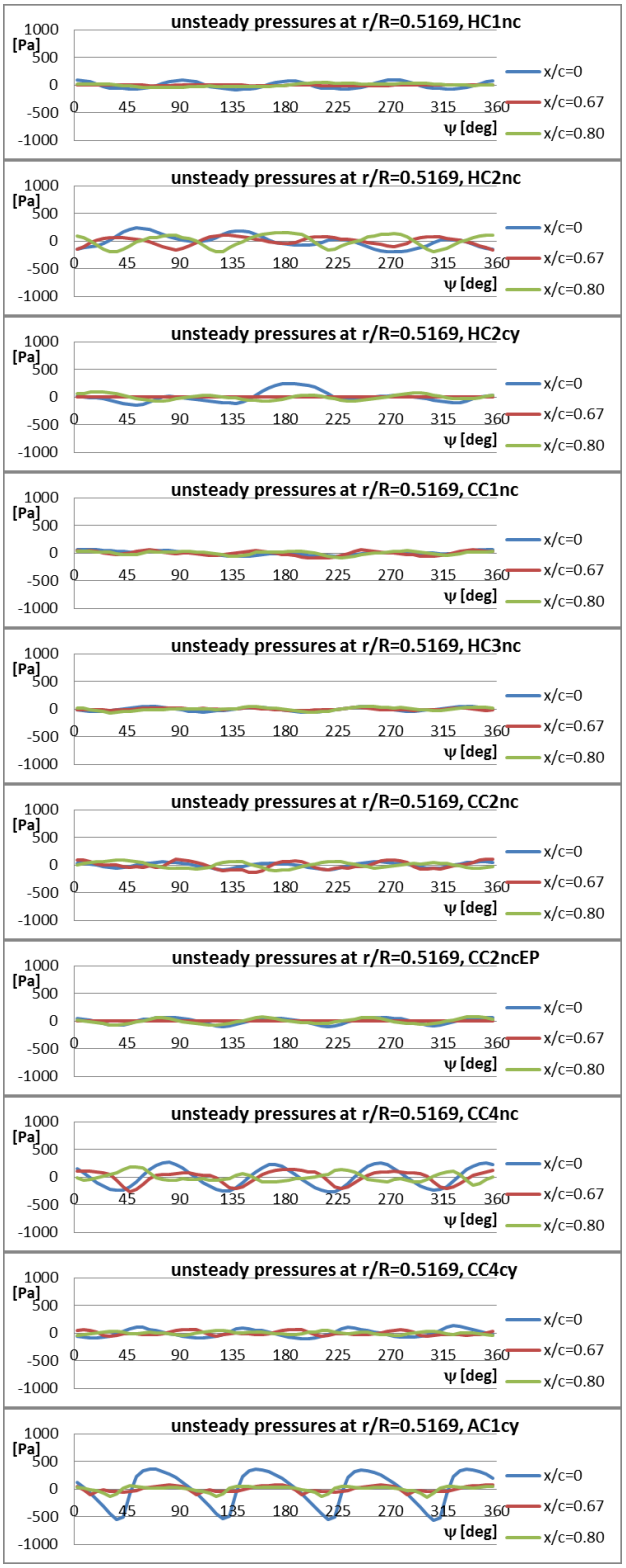

Figure 11: Unsteady pressures at span wise position 2y/b=0.5169, r/R=0.5169, different model configurations

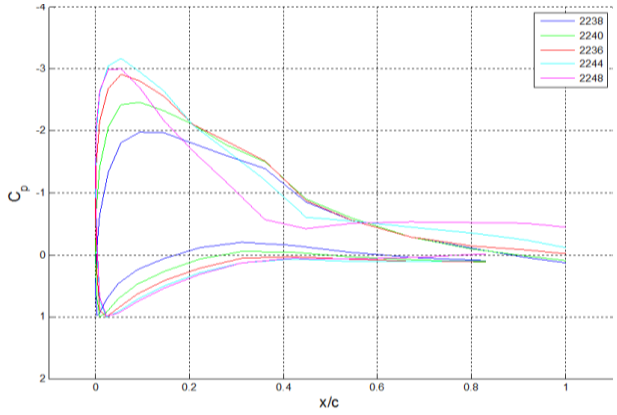

Figure 12: Pressure distributions at wing section LW-B (2y/b=0.3267), for AC1 case and α between 4.1 to 14.2 deg.

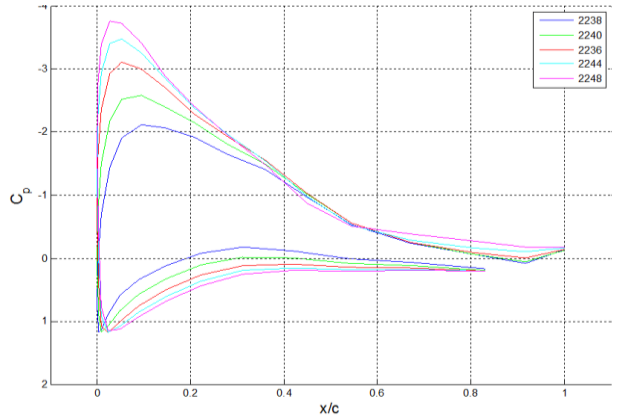

Figure 13: Pressure distributions at wing section LT-B (2y/b=0.6367), for AC1 case and α between 4.1 to 14.2 deg.

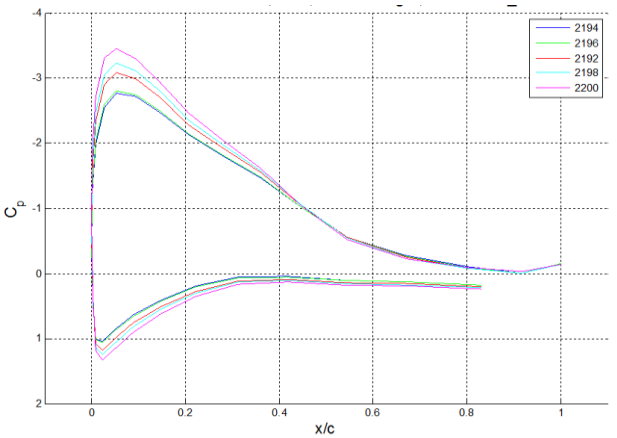

Figure 14: Pressure distributions at wing section LT-B (2y/b=0.6367, r/R=0.7365), for AC1 case and thrust from -90 to 750 N.

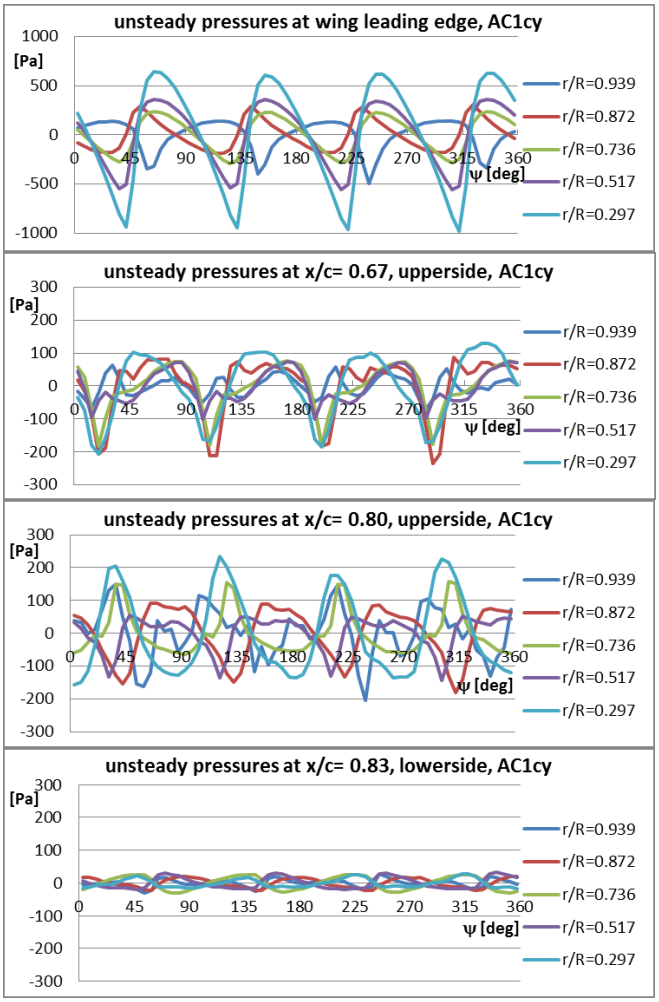

Figure 15: Unsteady pressures at all stream and span wise positions, AC1 trimmed condition.

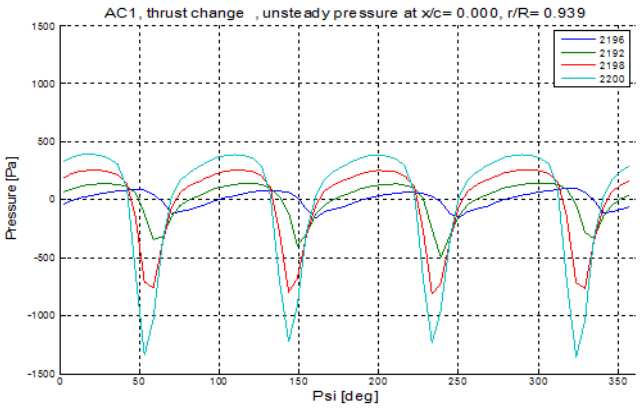

Figure 16: Unsteady pressures at wing LE, at r/R= 0.939 for thrust settings -43 N (dark blue), 277 N (green, trimmed), 500 N (red) and 750 N (light blue).

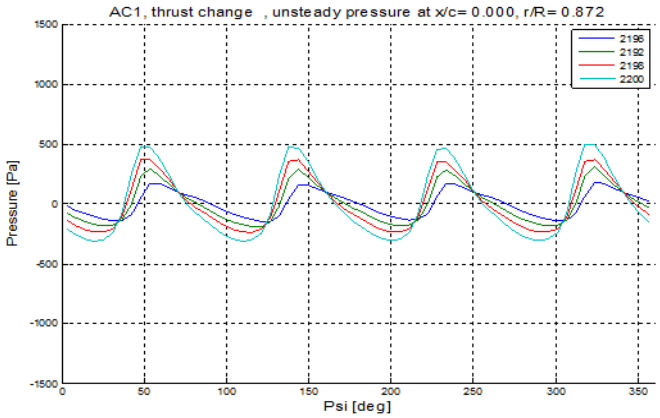

Figure 17: Unsteady pressures at wing LE, at r/R= 0.872 for thrust settings -43 N (dark blue), 277 N (green, trimmed), 500 N (red) and 750 N (light blue).

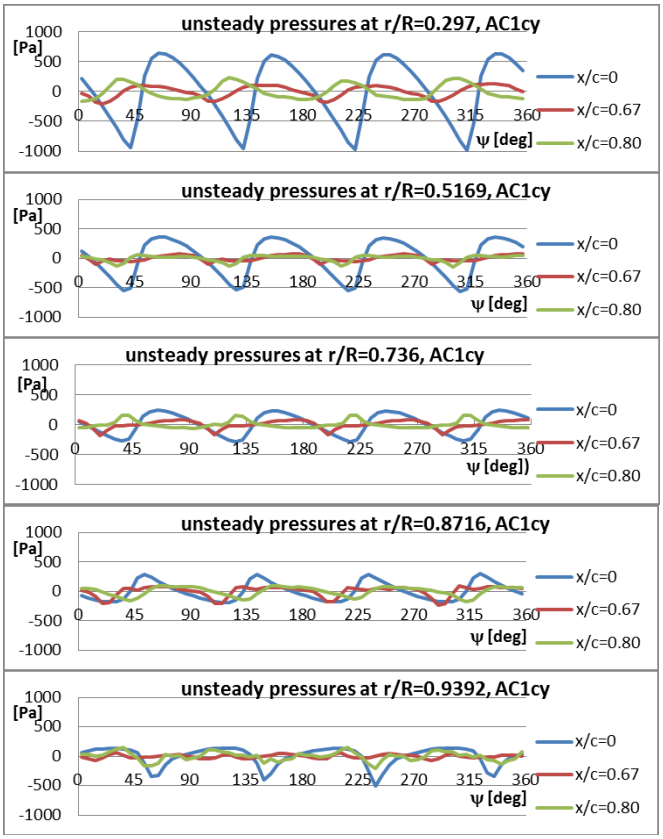

Figure 18: Unsteady pressures on all span wise positions on the upper side of the wing for AC1, trimmed condition.

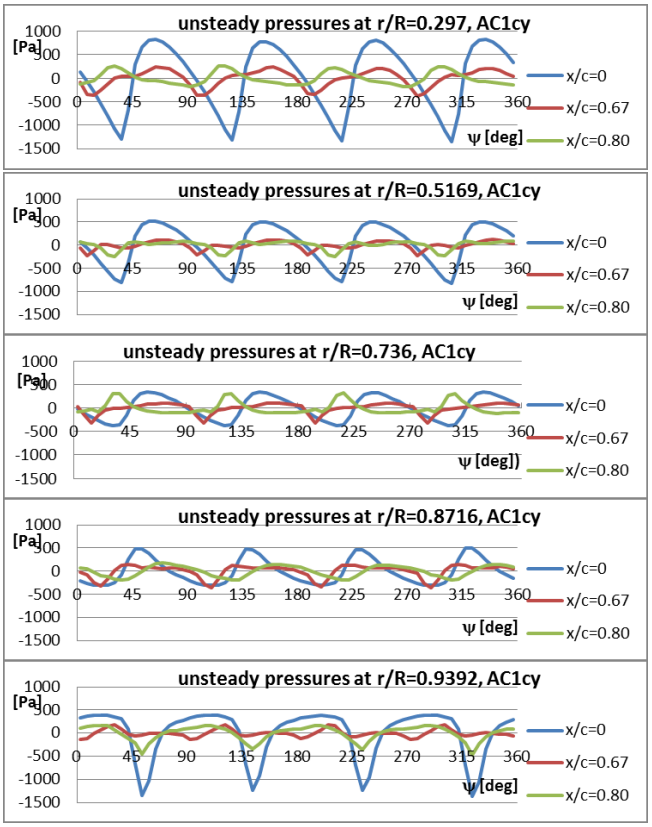

Figure 19: Unsteady pressures on all span wise positions on the upper side of the wing for AC1 at high thrust condition (715 N).

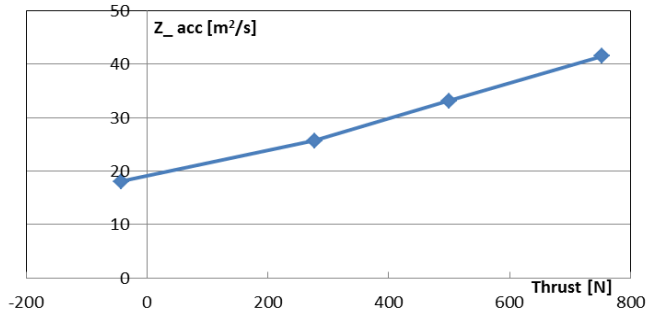

Figure 20: 4/rev vertical acceleration amplitude of the nacelle, depending on the thrust setting in AC1 configuration

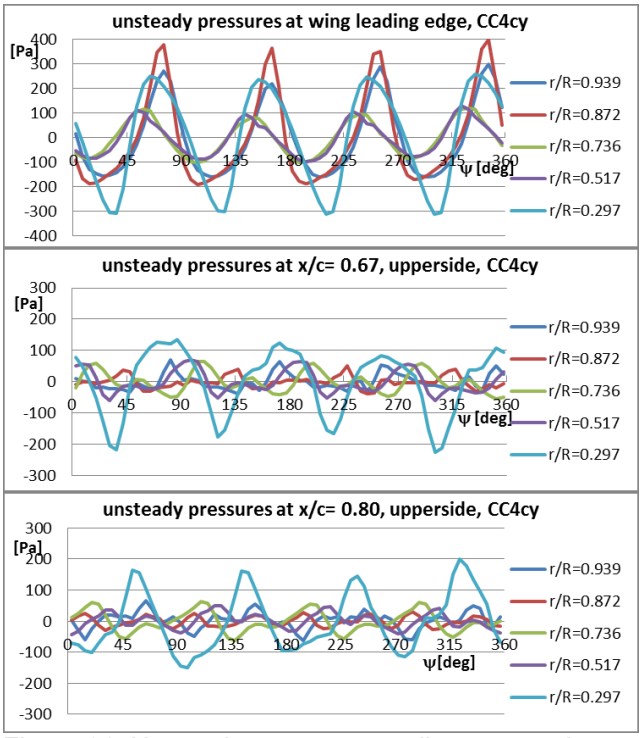

Figure 21: Unsteady pressures at all stream and span wise positions, CC4cy trimmed condition.

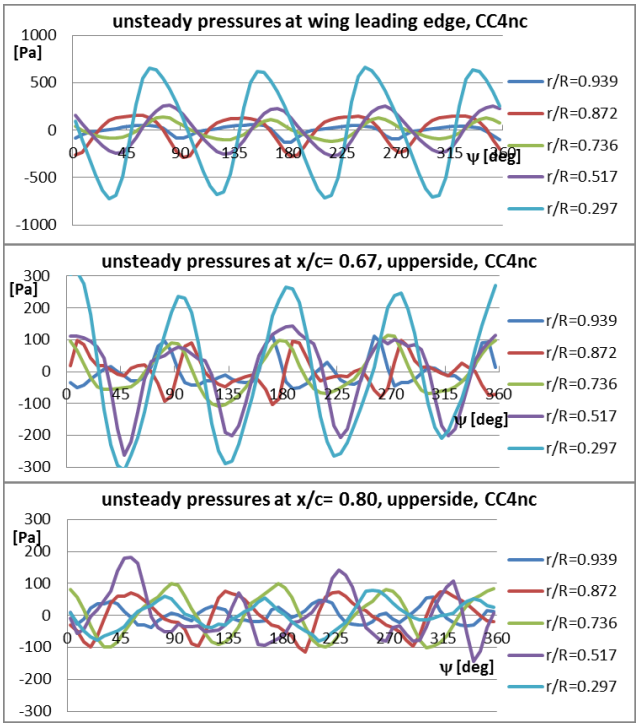

Figure 22: Unsteady pressures at all stream and span wise positions, CC4nc, trimmed condition.